View metadata, citation and similar papers at core.ac.uk
brought to you by CORE
provided by Purdue E-Pubs

Sixth International Conference on Durability of Concrete Structures **Paper Number PSE12**
18 - 20 July 2018
University of Leeds, Leeds, West Yorkshire, LS2 9JT, United Kingdom

Sulfate Resistance Study of Carbonated Low-Calcium Silicate Systems

R. Tokpatayeva and J. Olek
Lyles School of Civil Engineering, Purdue University, West Lafayette, IN, USA

J. Jain, A. Seth and N. DeCristofaro
Solidia Technologies Inc., Piscataway, NJ, USA

ABSTRACT

This paper summarizes the results of sulfate resistance study of carbonated mortar specimens made with Solidia Cement™ (SC) and tested for expansion according to ASTM C1012 specification while exposed to three types of soak solutions: sodium sulfate, magnesium sulfate and deionized water. A control set of ordinary portland cement (OPC) mortars was also evaluated. Besides the length change measurements, visual observations of changes in the appearance of specimens were conducted after various lengths of exposure. In addition, microstructural characterization of the specimens was conducted using scanning electron microscopy (SEM), X-ray diffraction (XRD) and thermo-gravimetric analysis (TGA) techniques. Finally, changes in the concentration of the chemical species present in the soak solutions in contact with the SC specimens were evaluated using both, the ion chromatography (IC) and the inductively coupled plasma optical emission spectrometry (ICP-OES).

As expected, the OPC mortar specimens started deteriorating early and reached the critical (i.e.0.1%) level of expansion in about 4 months in case of sodium sulfate solution and in about 6 months in case of magnesium sulfate solution. With respect to the SC mortar specimens, those exposed to magnesium sulfate solution showed higher expansion than those exposed to sodium sulfate solution. However, after 18 months of exposure to both types of sulfate solutions the maximum expansion levels of specimens were still only about 33% of the critical (value.

The SEM examination of SC mortar bars indicated that the matrix of the specimens exposed to magnesium sulfate solution showed evidence of formation of gypsum and magnesium-silica compounds. Magnesium and sulfate ions seem to have altered the morphology of the carbonation-generated silica phase and produced gypsum deposits in the air-voids, within the matrix and at the paste – aggregate interfaces. The formation of gypsum in those specimens was confirmed by the results of thermal and XRD analyses. Finally, the ionic analysis of the magnesium sulfate soak solution indicated consumption of sulfate ions whereas the concentration of the sulfates in sodium sulfate soak solution didn't change during the exposure period.

Keywords: low-calcium-silicate cement, aqueous carbonation, sulfate resistance

1.0 INTRODUCTION

The carbonation reactions have been used in the past to increase the rate of strength development of hydraulic calcium silicates (i.e. $3CaO{\cdot}SiO_2$ (C_3S) and β-$2CaO{\cdot}SiO_2$ (β-C_2S)) (Young *et al.*, 1971, Goto *et al.*, 1995) and to explore the potential for using non-hydraulic calcium silicates (e.g. γ-$2CaO{\cdot}SiO_2$ (γ-C_2S) and $CaSiO_3$ (CS)) as carbon dioxide (CO_2) activated binders (Bukowski and Berger, 1979). More recently, long-term sequestration of CO_2 by carbonation of naturally occurring calcium silicates emerged as a promising technology to curb raising levels of carbon dioxide is the Earth's atmosphere (Huijgen and Comans, 2005). The Solidia Cement™ (SC), developed by Solidia Technologies Inc., illustrates the case of implementation of carbonated calcium silicate as a binding medium in concrete. SC is a low-lime calcium silicate-based cement which can be produced in the conventional cement kiln and which requires lower clinkering temperature (~1200°C) compared to the clinkering temperature of the OPC (~1450°C).

The response of the OPC system to sulfate solutions has been widely studied and the basic mechanisms are reasonably well established. As an example, according to Taylor (1997), the monosulfate present in the matrix located in the interior of the hydrated OPC specimens exposed to sodium sulfate solution

gets replaced by microcrystals of ettringite thoroughly intermixed with calcium silicate hydrate (C-S-H). Closer to the surface, the formation of gypsum (both in the form of veins parallel to the surface as well as microcrystals intermixed with C-S-H) was also observed (Santhanam *et al.* (2002), Bonen and Cohen (1992)). The same authors also reported that the matrix of OPC exposed to magnesium sulfate solution will experience higher degree of decalcification than that observed in the case of exposure to sodium sulfate solution. In addition, the surface of the OPC specimens exposed to magnesium sulfate solution will typically develop a thin coat of composite material consisting of an outside layer of brucite ($Mg(OH)_2$) and underlying layer of gypsum. In addition, in cases of a very severe attack involving magnesium sulfate solution, formation of the non-binding magnesium silicate hydrate was also observed.

Despite sizeable amount of work on CO_2 sequestration in the calcium silicate systems, little can be found in the literature regarding the potential performance issues associated with the carbonated calcium silicate systems exposed to sulfate containing environment. In contrast, sulfate durability has been studied for other silicate systems alternative to OPC (for example, Słomka-Słupik *et al.* (2016), Duda (1987), Bakharev (2005)).

Due to previously mentioned lack of data on the sulfate durability of carbonated low-lime silicate systems, the objective of the presented work was to investigate the expansion potential of such materials upon exposure to sulfate-bearing solutions and to compare it to the behavior of the OPC system exposed to the same solutions. In addition, microstructural and chemical changes resulting from sulfate exposure were also evaluated.

2.0 MATERIALS AND METHODS

This paper presents analysis of two cementitious systems: hydrated OPC and carbonated SC.

2.1 Materials

The mortar specimens (25mm x25mm x285 mm prisms) were prepared using both, SC and OPC (Type I) cements and the ASTM C778-13 graded standard sand (Ottawa sand). The SC mortar bars were prepared using the w/c=0.30 and cement to carbonation was achieved by continuously purging the chamber with high purity CO_2 gas supplied at the pressure of 1 atm. The OPC mortar samples were prepared according to ASTM C109-12. After demolding, the OPC specimens were cured in saturated lime water at 23°C for 28 days. No such treatment was provided to the SC mortar bars since these do not require any post curing.

The chemical compositions of both, OPC and SC are given in Table 1. The main mineral phases present in SC cement (determined by XRD) include rankinite, pseudowollastonite and larnite/belite (reactive phases), and melilites and feldspars (inert phases). The XRD patterns of SC cement before in after carbonation are presented in Results section. The 0.35M sulfate solutions used in the experiment were prepared using analytical grade chemical reagents (anhydrous sodium sulfate and anhydrous magnesium sulfate).

2.2 Methods

Experimental setup for length change measurements

The sulfate exposure experiment was performed according to the ASTM C1012-13. All mortar bars were exposed to 0.35M solutions of sodium sulfate and magnesium sulfate with solid-to-solution volume ratio as 1:4 at 23°C. Mortar bars soaked in de-ionized water were used as reference specimens. The measurements of change in the length and the mass of the bars were performed at different time intervals (1, 2, 3, 4, 8, 11, 13, 15 weeks and 4, 6, 9, 12, 15 and 18 months). In addition, changes in the chemical composition of the soak solutions were evaluated after 8, 16 and 32 weeks of exposure. Before starting the soaking process, all SC mortar bars were pre-saturated in de-ionized water for 48 hours.

Length change measurements were performed after previously outlined period of exposure using the length comparator equipped with digital gauge with the resolution of 0.0025 mm. The percentage of the length change was calculated according to ASTM C1012. In addition, once the specimens were removed from the soak solutions for length and mass measurements they were also photographed to document changes in their physical appearance the mortar bars were recorded.

Table 1. Chemical compositions of Type I OPC and SC

OPC (Type I)											
Component	CaO	SiO_2	Fe_2O_3	Al_2O_3	MgO	SO_3	Total alkalis	C_3S	C_2S	C_3A	C_4AF
Wt, %	64.0	19.6	2.9	5.2	2.6	3.3	0.7	63.4	8.4	9.0	8.7
Solidia Cement™											
Component	CaO	SiO_2	Fe_2O_3	Al_2O_3	MgO	SO_3	Na_2O	K_2O	TiO_2	SrO	P_2O_5
Wt., %	43.6	44.0	1.79	5.13	1.15	0.16	0.33	1.94	0.22	0.12	0.06

Post-exposure analysis of the mortar bar specimens

After completion of the 18-month-long sulfate resistance test, both, the SC and OPC mortar bars (1 bar/per each solution) were dried at 50°C in vacuum oven and used to prepare the test specimens for XRD, TGA and SEM analyses.

XRD analysis

For XRD analysis, SC cement, pulverized small pieces of SC paste, SC and OPC mortar samples (removed from several locations) were used. Before being mounted in the XRD sample holder, ground samples were sieved using the No. 200 (75µm) sieve. The XRD patterns were collected using Siemens D500 diffractometer (30 mA, 50 kV) at 0.02°/sec scanning rate (in 10-80° 2θ range). The analysis of the pattern was performed using the Jade 9 software.

Thermal analysis

The SC and OPC powders utilized for XRD analysis were subsequently subjected to thermogravimetric analysis (TGA). The TGA analysis was performed using TA Instruments Q50 Thermogravimetric analyzer with the nitrogen gas atmosphere (the flow rate of 50 mL/min) in the temperature range from 20°C to 1000°C at the heating rate of 10°C/min.

SEM analysis

The specimens for SEM observation were prepared by cutting the bar at two locations (~ 15 mm apart) in the direction perpendicular to the longitudinal axis (see Fig.1). This resulted in the 20 mm thick specimen with the 25mm x 25mm area that was used for conducting the SEM analysis. Once cut out of the beam, the

cube specimens were vacuum impregnated with epoxy and dried at ~60ºC. After the epoxy hardened, the surface of the specimens was ground using Hillquist 45, 30 and 15 µm mesh flat diamond laps. Lapped samples were subsequently polished on Buehler microclothes lubricated with diamond pastes with mesh sizes of 9, 6, 3, 1 and 0.25 µm. The SEM analysis was performed using the ASPEX Personal SEM equipped with the energy dispersive x-ray (EDX) analyzer and operated in the backscattered and secondary electron modes. The accelerating voltage used in the examination was 15 keV.

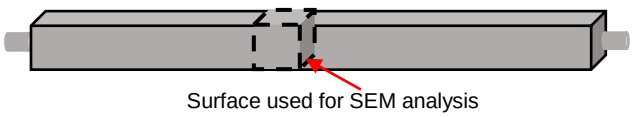

Fig. 1. Location of SEM specimen

Chemical analysis of the soak solutions of SC specimens

The soak solutions (de-ionized water, magnesium sulfate and sodium sulfate solutions) that remained in contact with SC mortar bars during the testing period were collected at various intervals during the exposure cycle and analyzed to monitor the changes in concentration of Na^{+}, Mg^{2+}, Ca^{2+}, SO_4^{2-} and Si species. The solutions were filtered and analyzed using Ion Chromatographer (IC) (DIONEX ICS-900) and Inductively Coupled Plasma – Optical Emission Spectrometer (ICP-OES) (Perkin Elmer OPTIMA 8300). The ion concentration results reported here represent an average of two samples per each solution.

3.1 RESULTS

3.1 Length change and visual observation results

As it can be seen from Fig.2, the appearance of the SC mortar bars did not change during the entire (i.e. 18 months) exposure period. However, the mortar bars made from the OPC and exposed to the sodium sulfate solution developed severe bending, which ultimately led to two of them becoming completely broken after 9 months of exposure. On the other hand, in case of the OPC mortar bars exposed to magnesium sulfate solution such symptoms as exfoliation, formation of brucite deposits (white precipitates) and slight bending were observed (right part of Fig. 3). The SC mortar specimens exposed to magnesium sulfate solution (left side of Fig. 3) initially developed hairline cracks along the length of the bars which, over time, spread toward the end corners of the bars (Fig. 4). The summary of visual observations of the conditions of the bars is presented in Table 2.

Figures 5 (a, b) and 6 (a, b) show the values of length change measurements for all SC and OPC mortar bars exposed to, respectively, the sodium sulfate (SS) and magnesium sulfate (MS) solutions. In general, regardless of the type of the sulfate solution used, the maximum expansion of the SC mortar bars after 72 weeks (~18 months) of exposure was very low (~0.03%). That maximum expansion was observed in the bars immersed in magnesium sulfate solution. The maximum expansion limit (at 180 days or ~26 weeks) for moderate sulfate exposure specified in the ACI 201.2R-16 is 0.1%. According to that, the SC bars can be definitely considered to be resistant to the distress caused by the sulfate sources external to the concrete.

Fig. 2. Appearance of the mortar bars exposed to sodium sulfate (SS): left – SC mortar bars after 18 months of exposure; right – OPC mortar bars after ~9 months of exposure

Fig. 3. Appearance of the mortar bars exposed to magnesium sulfate (MS): left – SC mortar bars after 18 months of exposure; right – OPC mortar bars after ~9 months of exposure.

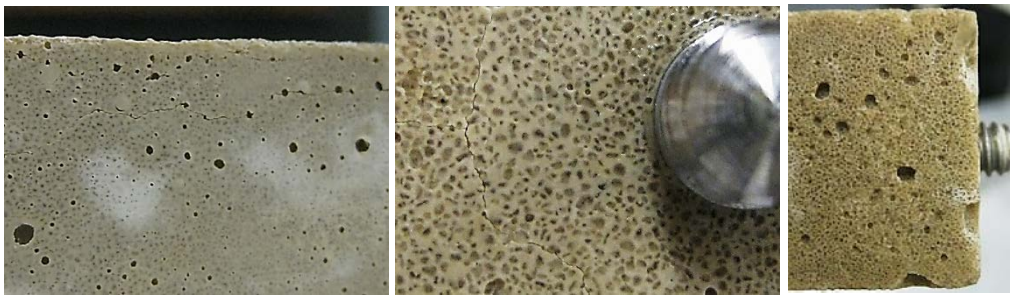

a) b) c)

Fig. 4. Cracks on the surface of SC mortar bar exposed to magnesium sulfate (MS) solution (0.35M): a) – longitudinal cracks on the top of the vertical face in the region close to the finished surface; b) – crack at the end face of the bar near the steel stud; c) – side view of the crack on a vertical face near the end of the bar

Table 2 Summary of visual observations of the condition of mortar bars exposed to sulfate solutions

Solution	OPC mortar	SC mortar
Sodium sulfate (SS)	✓ 3 of the bars cracked and broke (test have been terminated after 6 months) ✓ Cracks appeared mostly near the corners, along the edges and along sides close to the finished surface; ✓ A network of cracks developed along the long sides of the bars near the end of the test	✓ No visible changes
Magnesium sulfate (MS)	✓ All bars bent and cracked after 12 months of exposure ✓ The surfaces of the bars were covered with white deposits; ✓ Edges became blunt due to crumbling of sand particles.	✓ Fine horizontal cracks started to propagate along the length of the bar in the region close to the finished surface ✓ Cracks started to propagate along the ends and corners of the bars after about 14-15 months of exposure (See Fig.4).

However, as it can be seen in Figs. 5 (b) and 6 (b), the OPC mortar bars expanded beyond the critical level after, respectively, 4 months of exposure to sodium sulfate solution and 6 months of exposure to magnesium sulfate solution. In fact, the test involving the OPC specimens had to be terminated due to severe cracking and disintegration of the bars. Also, it is worthwhile to point out the 2-stage expansion trend of the OPC mortar specimens exposed to sodium sulfate characterized by relatively moderate initial expansion (stage 1) and rapid acceleration of the expansion (stage 2). This phenomenon was previously described by Santhanam *et al.* (2002). These authors suggested that the sudden acceleration of expansion observed during stage two can be the result of increased rate of formation of gypsum and ettringite. The expansion of SC mortar bars exposed to both magnesium sulfate and sodium sulfate solutions stabilized after 48 and 32 weeks of exposure respectively. However, the SC mortar bars exposed to magnesium sulfate experienced a higher total length change (~0.03%) as compared to the total length change of ~0.015% observed for the SC mortars exposed to sodium sulfate.

Figure 7 presents the detailed comparison of average length change values of the SC mortar bars immersed in de-ionized water, sodium sulfate and magnesium sulfate solutions. As one can observe from the graph, the SC specimens exposed to magnesium sulfate solution behaved differently than those exposed to de-ionized water and sodium solution. Specifically, after approximately 36 weeks of exposure the expansions of specimens exposed to deionized water and sodium sulfate solutions stabilized at about 0.015%. However, the SC mortars exposed to magnesium sulfate solution continued to expand, reaching a steady level of expansion (~0.03%) only after about 48 weeks of exposure. Even though (as it has been mentioned above) all SC mortar specimens passed the maximum length change (expansion) criterion, the bars exposed to magnesium sulfate expanded significantly more compared to those exposed to sodium sulfate solution. This observation suggests that magnesium sulfate solution may have some chemical effect that changes the structure of the specimens. The microstructure of the SC mortar specimens after sulfate exposure provided some confirmation of this observation. The results of the microstructural study are presented and discussed in the following paragraphs.

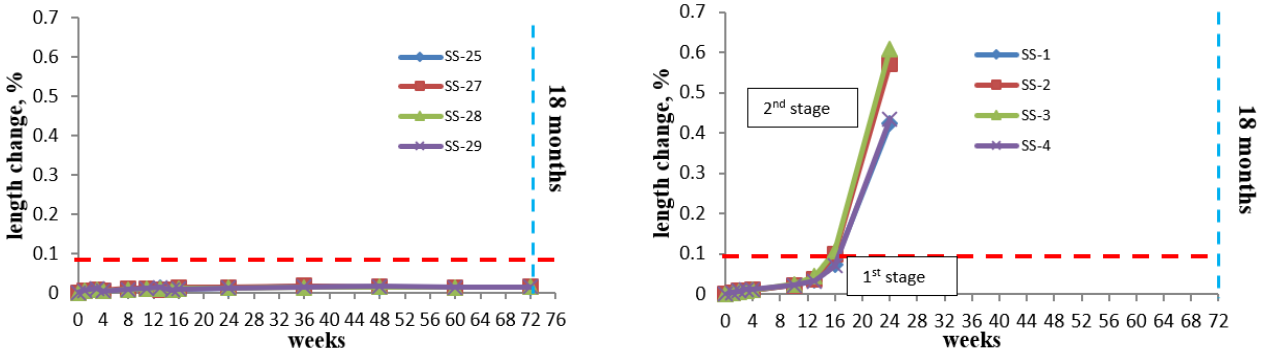

a) SC mortar bars a) OPC mortar bars

Fig. 5. Length change results for the SC mortar specimens exposed to sodium sulfate (SS) solution (Note: the horizontal dashed line represents the 0.1% maximum expansion limit (at 180 days or ~26 weeks) for moderate sulfate exposure as per ACI 201.2R-16)

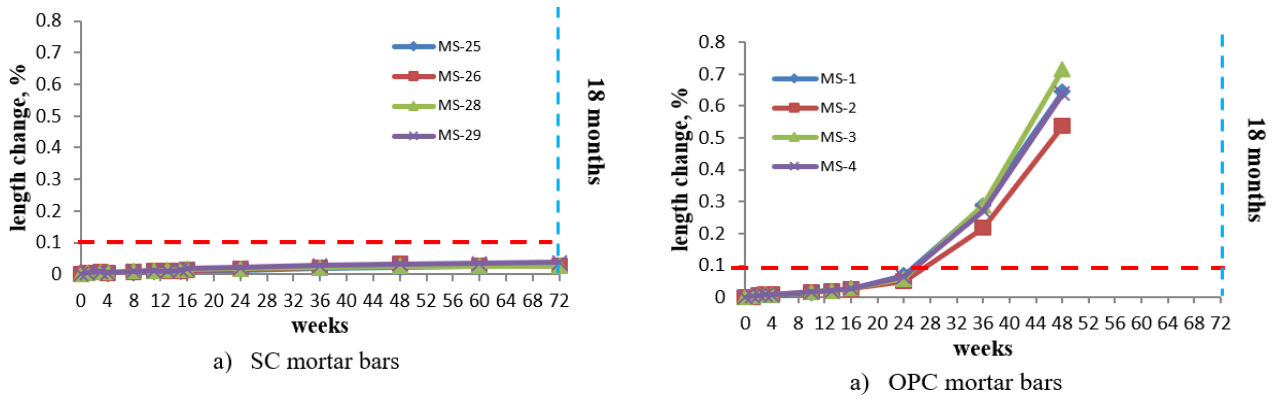

Fig. 6. Length change results for the OPC mortar specimens exposed to magnesium sulfate (MS) solution (Note: the horizontal dashed line represents the 0.1% maximum expansion limit (at 180 days or ~26 weeks) for moderate sulfate exposure as per exposure as per ACI 201.2R-16)

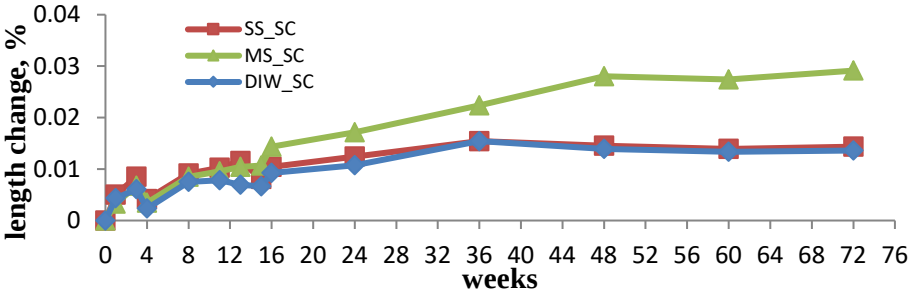

Fig. 7. Length change measurement results for SC mortar bars (key: DIW – de-ionized water, MS – magnesium sulfate, SS – sodium sulfate)

3.2 Results of SEM Analysis

The SEM analysis of the SC and OPC mortar specimens was used to evaluate the changes in the microstructure and examine the morphology of any new phases that might have formed as the result of the exposure of the matrix to sulfate solutions. In general, the microstructure of carbonated SC system consists of calcium carbonate, hydrated silica gel, unreacted cement grains and micro-/nano-pores (see Fig. 8). Calcium carbonate phases (calcite, vaterite and aragonite) are the main space-filling and binding components. In addition, the microstructure also contains an "intermediate phase" composed of silica gel and pure calcium carbonate. That phase can be described as "low-silica carbonate phase".

The formation of this type of intermediate phase might be due to multi-mineral nature of the SC cement. The layer of hydrated silica gel tends to deposit around the contours of un-carbonated grains of cement. As mentioned earlier, the SC contains non-reactive particles which act as an inert filler.

Figure 9 contains SEM images of the microstructure of both, the SC mortar bars (images (a) and (c)) and the OPC mortar bars (images (b) and (d)) exposed to either sodium sulfate (images (a) and (b)) or magnesium sulfate (images (c) and (d)) solutions. As it can be seen by comparing images shown in Fig. 9 (a) and (b), the sodium sulfate solution does not appear to have any significant negative effects on the microstructure of the carbonated SC system. The only observable change is the increase in porosity of the very near surface (about 1 mm deep) region of the specimen which might be due to dissolution and leaching of certain species (see section on soak solution analysis near the end of the paper). In contrast, the matrix of the OPC specimen exposed the same sodium sulfate solution is severely cracked. However, the microstructure of the SC mortar specimens exposed to magnesium sulfate looks deteriorated (Fig. 9 (c)) and the degree of deterioration appears to be similar to that observed in the matrix of OPC specimens exposed to the same solution (see Fig.9 (d)). It should be noted, however, that despite the observed microstructural changes the observed length changes of SC bars in the MS solution were very low.Fig.10 compares SEM images taken at the low (~18X) magnification from the matrices of the SC mortar bars exposed to three different solutions: the deionized water, the sodium sulfate solution and the magnesium sulfate solution. It can be observed that the top 1 mm of the specimen exposed to the sodium sulfate

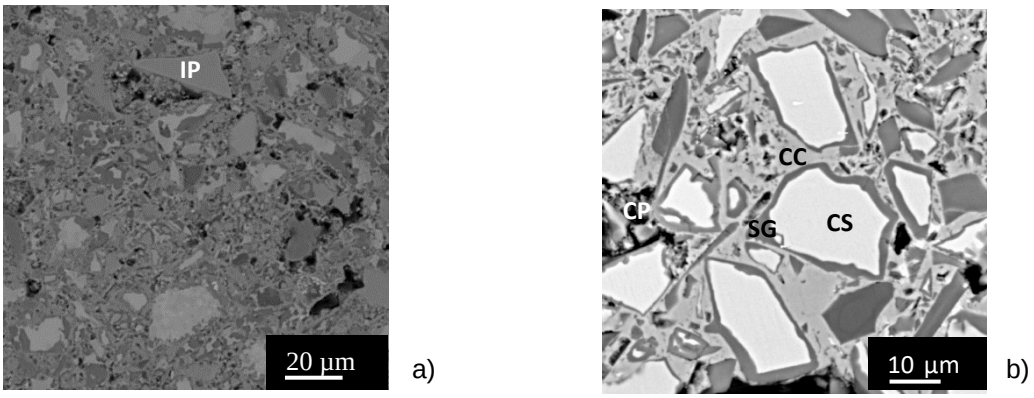

Fig. 8. SEM micrograph of SC paste matrix (key: CS – calcium silicate, SG – silica gel, CC – calcium carbonate, CP – capillary pore, IP – inert phase)

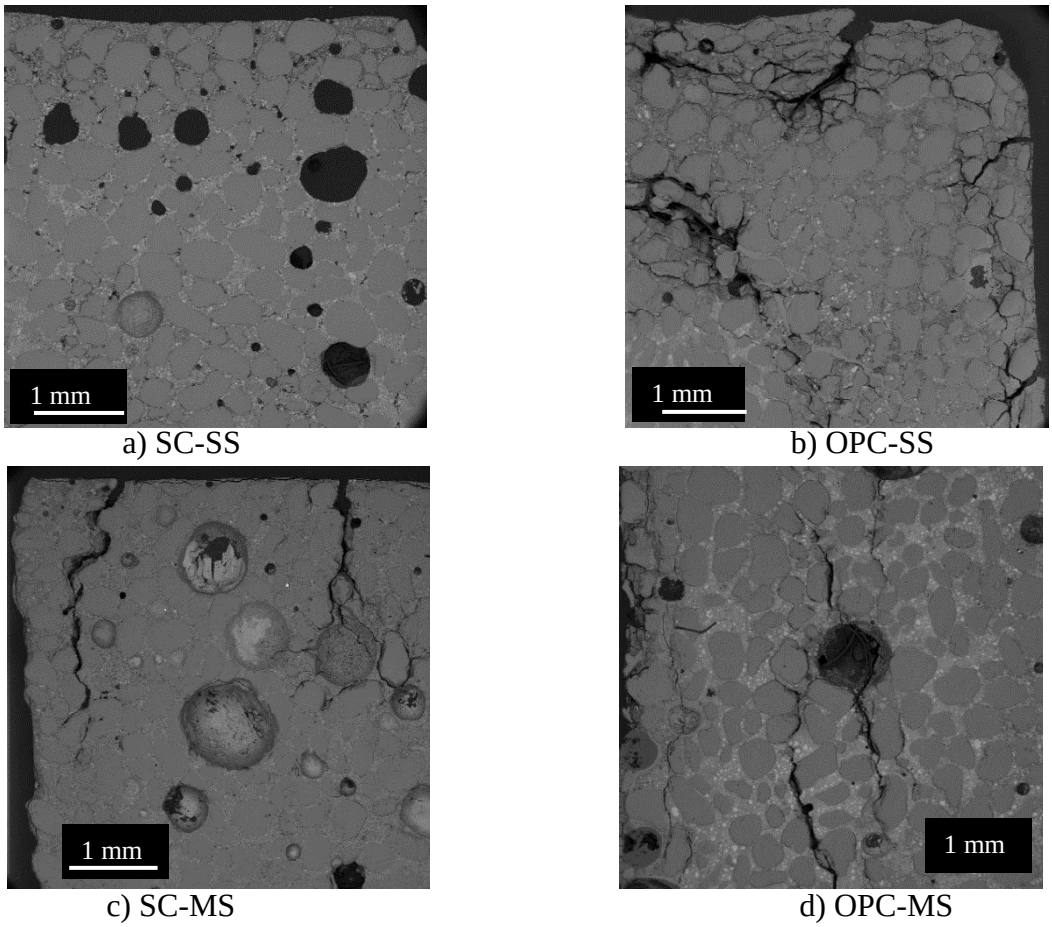

Fig. 9. Comparison of the microstructure of the mortar matrices after exposure to sodium sulfate solution (a – SC and b – OPC) and magnesium sulfate solution (c – SC and d – OPC).

solution (Fig. 10 (b)) appears to be more porous than the same region of the specimen exposed to deionized water. While the top region of the specimen exposed to the magnesium sulfate solution (Fig. 10 (c)) does not display any signs of increased porosity, it does contain a series of microcracks extending to the depth of about 2 mm from the surface of the bar. No cracks were observed in the microstructure of specimens exposed to the deionized water and to the sodium sulfate solution. When examined at higher magnification (~100X) the microstructure of mortar bar specimens exposed to magnesium sulfate solution displays several other alterations described below. First, the deposits of gypsum were observed in several locations within the matrix. Specifically, the gypsum crystals were found in the air-voids (see Fig. 11), at the aggregate – matrix interface (see Fig. 12) and in other random locations within the bulk of the matrix. The somewhat preferential deposition of gypsum at paste-aggregate interface might be the result of the availability of free space at this location (the interface regions tend to be more porous) and/or the presence at this location of high calcium reactive phase.

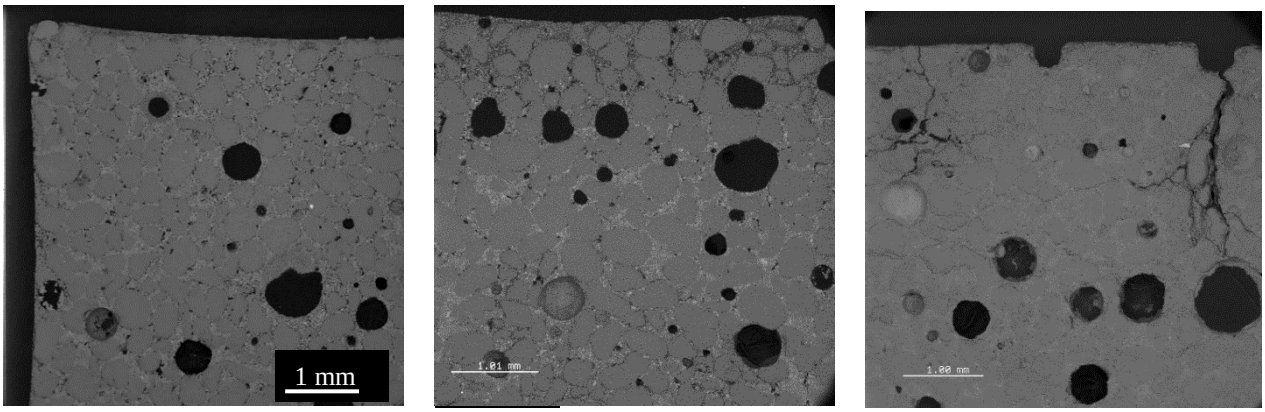

a) b) c)

Fig. 10. The SEM micrographs of the matrix of the SC mortar bars matrix collected at low magnification (18X): after exposure to a) deionized water, b) sodium sulfate solution, and c) magnesium sulfate solution

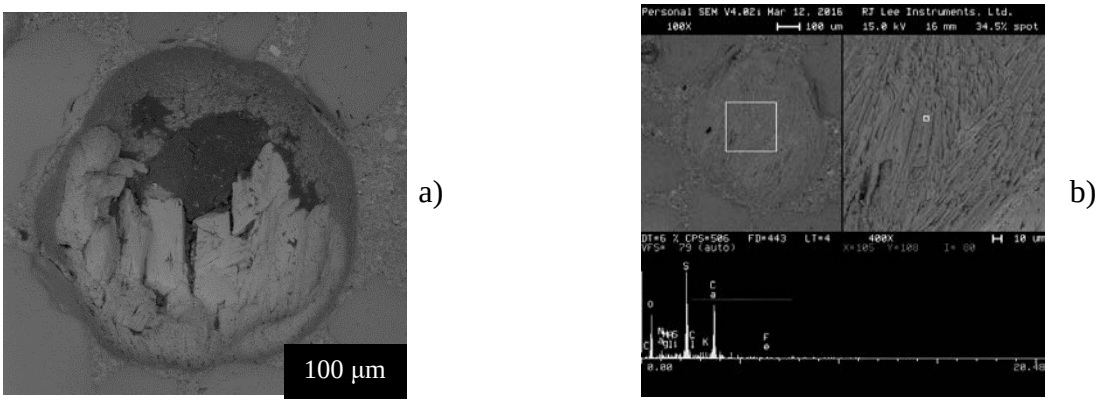

a) b)

Fig. 11. Higher magnification (~100X) SEM micrographs of the microstructure of the SC mortar bar matrix exposed to magnesium sulfate solution showing; (a) the air void partially filled with gypsum and (b) the air void completely filled with gypsum (composition confirmed by the EDX spectrum)

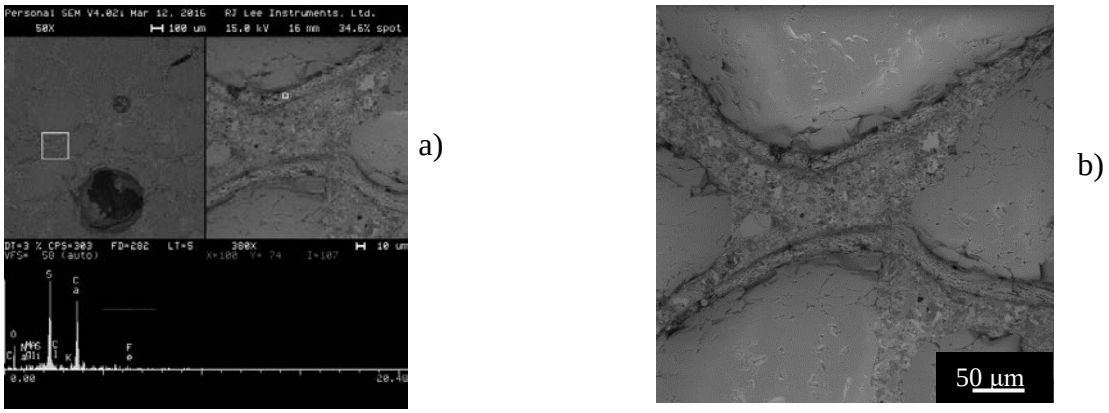

a) b)

Fig. 12. The SEM images of the microstructure of the SC mortar bar matrix exposed to magnesium sulfate solution showing: (a) the deposits of gypsum at the interface between the matrix and the aggregate and (b) the close-up of the interfacial zone with the veins of gypsum surrounding the aggregate particles

Other alteration of the matrix observed in the SC mortar bars exposed to magnesium sulfate solutions involved decalcification (Fig. 13 (a)) and infusion of silica gel with the Mg^{2+} ions (Fig. 13 (b)). More specifically, the magnesium ions were found both, within the silica gel as well as in the non-carbonated cement particles (where it was substituting for Ca^{2+}). As demonstrated in Fig. 13 (b), one can see Mg-Si-O signal originating from the silica rim of the carbonated calcium silicate particle. This might be interpreted as a formation of magnesium-silicate hydrate type gel, similar to that observed to form in the hydrated OPC system exposed to magnesium containing solutions. However, there is a significant difference in morphology of the affected regions in the SC and

the OPC systems as can be seen by comparing the images shown in Fig. 14 (a) and (b). Specifically, the replacement of the Ca^{2+} ion by Mg^{2+}in the matrix of the SC does not seem to have any visible damaging effects. On the other hand, the formation of magnesium-silicate-hydrate (MSH) type of product in the matrix of the OPC mortar

3.3 XRD Analysis results

As seen in Fig. 15 (lower trace) the main reactive crystalline phases present in SC cement before carbonation include rankinite, pseudo-wollastonite and larnite/belite. The main non-reactive phases include gehlenite (melilite family) and feldspars. After carbonation, peaks of calcium carbonate minerals appear as well as the peak intensity of the reactive phases decrease (see Fig. 15 upper trace). Fig.16 shows the XRD pattern of SC mortar specimens exposed to de-ionized water, sodium sulfate and magnesium sulfate solutions. The results of the XRD analysis didn't show any significant differences in the mineralogy of the specimens immersed in de-ionized water and sodium sulfate solution (other than decrease in the height of the calcite peaks in specimens exposed to SS). This might be attributed to the dissolution of calcite phase which was evidenced by SEM results as an appearance of less dense area close to the surface of the specimen bar resulted in cracking On the other hand, the XRD pattern of the specimen exposed to magnesium sulfate revealed the peaks of gypsum, in agreement with SEM results. In addition to that, one can notice that the intensities of the peaks for calcite were significantly lower than those observed in the specimen exposed to the de-ionized water. The slightly acidic pH level of the magnesium sulfate solution (~5-6) may accelerate the dissolution of the calcite phase compared to other soak solutions used in this study. Thus, the affected calcite phase may be the source of calcium ions for the formation of gypsum. Moreover, it is also interesting to note that the vaterite peaks appeared to be more pronounced in the specimens exposed to both types of sulfate solutions. In the specimens exposed to de-ionized water, any initially presented vaterite (also, amorphous calcium carbonate, if any) might have been converted into calcite. This may explain relatively higher intensity calcite peaks observed in these specimens. The studies conducted in biomineralization area (and mimicking of the synthesis of the less stable calcium carbonate polymorphs) suggests that the presence of organic macromolecules (e.g. proteins, polysaccharides, etc.) and different ionic species (e.g., ammonia, phosphates, sulfates, silica, etc.) during the precipitation event may extend the time of phase

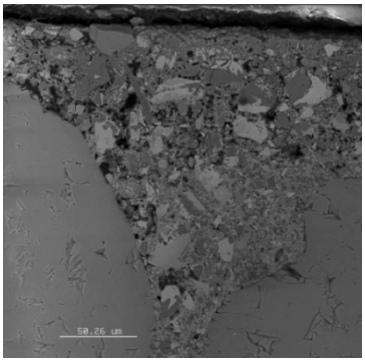

a)

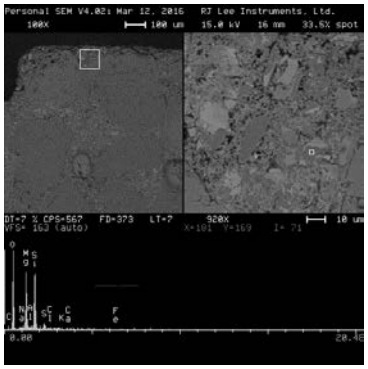

b)

Fig. 13. The SEM images of matrix of the SC mortar bar specimen exposed to magnesium sulfate solution; (a) the decalcified (porous) zone located close to the outer surface of the specimen and (b) the EDX signal indicating the presence of the Mg^{2+} inclusions in the silicate rim of partially-reacted cement particle.

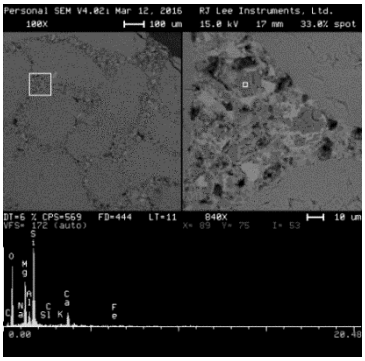

a)

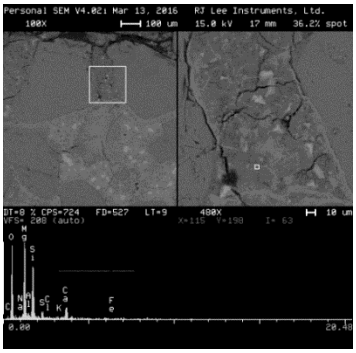

b)

Fig. 14 Comparison of the effects of the formation of the MSH-type phase in: (a) the SC and (b) the OPC mortar samples exposed to magnesium sulfate solution

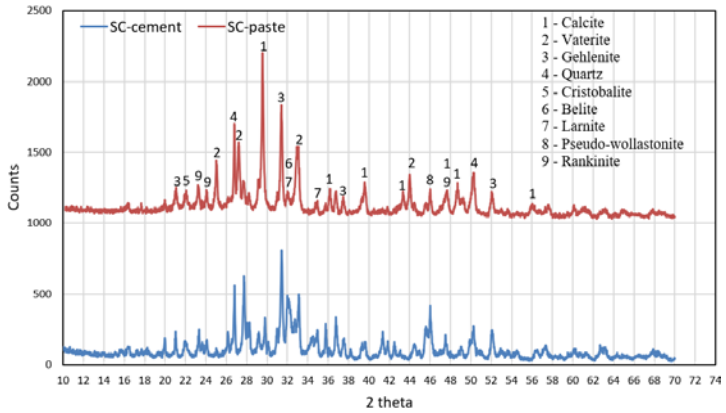

Fig. 15. The XRD patterns of SC cement (lower trace) and carbonated SC paste (upper trace)

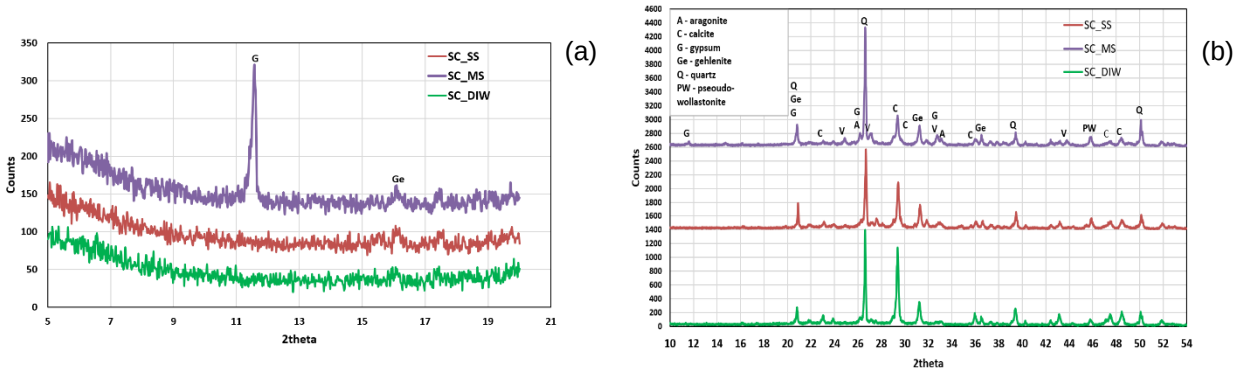

Fig. 16. The XRD patterns of SC mortar bar specimens after 18-month exposure to the de-ionized water, sodium sulfate and magnesium sulfate solutions; key: SC – Solidia cement, DIW – de-ionized water, SS – sodium sulfate, MS – magnesium sulfate); (a) – 5°-20° 2 theta range, (b) –10°-54° 2 theta range

transformation and/or help to keep those phases unchanged (Kirboga and Oner (2013), Popescu *et al.* (2014) and Fiori *et al.* (2009)). Magnesium ion is believed to act as a preservation agent for amorphous calcium carbonate phase and vaterite according to research work done by Ma and Feng (2015) and Lowenstam and Abbot (1975).

Lastly, as it can be seen from Fig. 16 (b), carbonated system exposed to sulfate did not contain any AFt/AFm phases (most likely because alumina present in this cement is incorporated in the non-reactive gehlenite.

3.4 Results of Thermal Analysis

The results of the thermogravimetric analysis (TGA) of the SC mortar specimens are given as a first derivative of weight change thermogram in Fig. 16. According to the curves, there is a reduction in the quantity of highly crystalline calcium carbonate (present in the temperature range of 650°-900°C) in mortar bars exposed to both sodium and magnesium sulfate solutions compared to the same mortars immersed in de-ionized water. This reduction is manifested by the shift of the TGA curve in the direction of lower temperature range and the appearance of the humps in between ~520°-650°C (encircled by the black dashed line in Fig. 17). The value of this reduction was estimated to be in the range of 30-35% (compared to the DIW (reference) sample). As mentioned above, the decomposition humps observed in the temperature range of ~520°-650°C might be attributed to the decomposition of less crystalline types of calcium carbonate and calcium bearing silica phases. In addition, the total amount of mass loss in the range of ~525°-900°C is lowest in case of the specimen exposed to magnesium sulfate solution. This implies that part of the calcium bearing phases was consumed during gypsum formation. The weight loss at the temperature of about 70°-150°C, visible in the curve of SC bars exposed to the magnesium sulfate, is attributed mainly to the dehydration of gypsum.

3.5 Results of chemical analysis of the soak solutions

The analysis of all soak solutions involved monitoring the levels of sulfate ions that could potentially be removed from the soak solution and incorporated (bound) within the matrix of the SC mortar specimens as well as the levels of Ca^{2+} ions and the dissolved silica which can migrate into the solution as the result of leaching. The pH values of the freshly prepared (i.e. not yet in contact with the mortar bars) sulfate solutions were in the range of ~5-6 for magnesium sulfate and ~7-8 for sodium sulfate solutions. When the solutions came in contact with the SC mortar bars, the pH values increased to the range of about 8.5-8.7 for

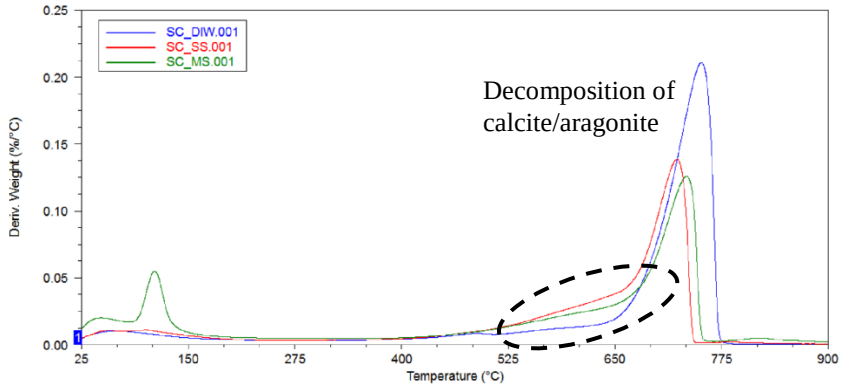

Fig. 17. The TGA curves of SC mortar samples: first derivative of weight (%) vs. temperature (key: DIW – de-ionized water, SS – sodium sulfate, MS – magnesium sulfate)

magnesium sulfate solution and up to about 10 for sodium sulfate solution. Changes in sulfate concentration within first 8 months of exposure (normalized with respect to the initial concentration in the fresh solutions) are plotted in Fig.18. The analysis of trends presented in Fig. 17 reveals that relative concentrations of the SO_4^{2-} ions, in the magnesium sulfate solution in contact with the SC mortar specimens decreased by about 20% compared the original concentration. These results can indicate that the sulfate ions were likely incorporated into the microstructure in the form of gypsum.

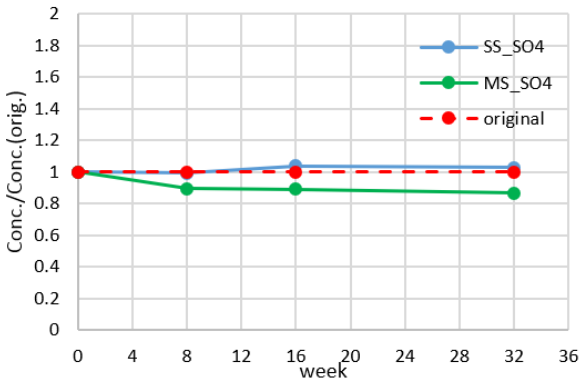

Fig. 18. Changes in the concentration of sulfate ions (SO_4^{2-}) in sulfate solutions in contact with the SC mortar bars (normalized with respect to e concentration of SO_4^{2-} in the original solution). (key: SS – sodium sulfate, MS – magnesium sulfate)

The graphs shown in Figs. 19 and 20 illustrate how the type of sulfate solution influences the amount of calcium and silica that can be leached out from the carbonated SC system. As seen in Fig. 19, the highest amount of calcium leached out of SC specimens exposed to magnesium sulfate solution. This can be explained by higher dissolving potential of the magnesium sulfate solution.

As for leaching of silica from the carbonated SC system after exposure to sulfate solutions, the amount present in the magnesium sulfate solutions was significantly (~8 times) lower compared to reference condition (i.e. the SC bars immersed in de-ionized water). This may indicate the presence of some chemical reactions which result in binding of silica in the microstructure.

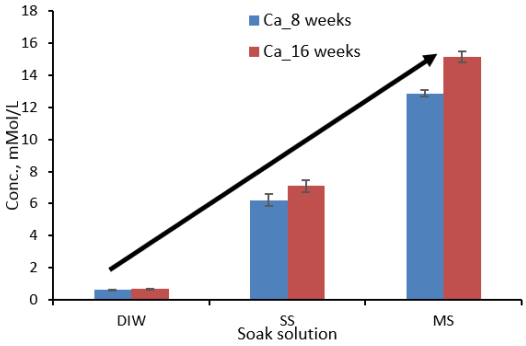

Fig. 19. Levels of calcium ions (Ca^{2+}) ions in various soak solutions in contact with the SC mortar bars for a period of 8 and 16 weeks (key: DIW – de-ionized water, SS – sodium sulfate, MS – magnesium sulfate)

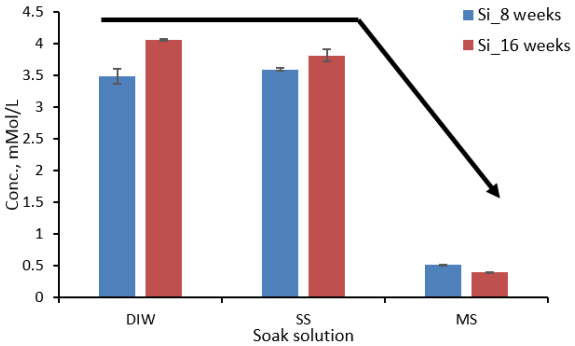

Fig. 20. Levels of silica (Si) in various soak solutions in contact with the SC mortar bars for a period of 8 and 16 weeks (key: DIW – de-ionized water, SS – sodium sulfate, MS – magnesium sulfate)

4.0 CONCLUSIONS

This paper contains the summary of the results of the 18-month long sulfate resistance tests performed on both, the carbonated SC and hydrated OPC mortar specimens according to modified ASTM C1012 standard. In general, the study indicated that the SC mortars are not negatively affected by the exposure to the sodium and magnesium sulfate solutions (i.e. this type of matrix was determined to be durable under sulfate exposure). When compared to the OPC system, the carbonated SC system has its own advantageous peculiarities, which help it to withstand the sulfate attack.

The following points briefly highlight the main findings of this study:

- At the end of the test period (i.e. 18 months) the SC mortar bar specimens did not reach the critical level of expansion (in fact their maximum expansion was only about 33% of the value of 0.1%). On the other hand, the OPC mortar bars not only exceeded the threshold value of expansion, but they also started to disintegrate after about 5-6 months of exposure.
- The results of multiple post-exposure tests (chemical analysis of soak solutions as well as the XRD, TGA and SEM analyses of solid phases) indicates importance of the cation present in sulfate solution. To be exact, there is a chemical interaction between the SC mortar matrix and the magnesium sulfate solution. This reaction resulted in partial decalcification of the SC matrix, in the reduction of more crystalline forms of calcium carbonate (calcite/aragonite), formation of gypsum, and incorporation of Mg^{2+}ions into the structure of silica. However, as mentioned earlier, this reaction did not seem to cause substantial expansion or have other destructive effect on the matrix.
- There were not significant effects of sodium sulfate solution on the microstructure of the SC mortar specimens with the exception of the slight increase in porosity of the thin (about 1 mm) near-surface region of the specimen and possible formation of less crystalline polymorphs of calcium carbonate (exposure to magnesium sulfate led to similar changes).
- The absence of calcium hydroxide and reactive calcium aluminates in the SC matrixes may be considered as one of the big advantages of this system with respect to its durability when exposed to external sulfate attack.

References

ACI 20.2R-16 Guide to Durable Concrete, ACI Committee 201.

ASTM Standard Designation C1012-13, Standard Test Method for Length Change of Hydraulic-cement Mortars Exposed to a Sulfate Solution, ASTM, PA, 2013

ASTM Standard Designation C109-12, Standard Method for Compressive Strength of Hydraulic Cement Mortars (using 2-in. [50 mm] Cube Specimens), ASTM, PA, 2013.

ASTM Standard Designation C778-17 Standard Specification for Standard Sand, ASTM, PA, 2017

Bakharev. T., “Durability of Geopolymer Materials in Sodium and Magnesium Sulfate Solutions”, *Cement and Concrete Research,* 35 (2005), pp. 1233-1246.

Bonen. D and Cohen. M.D., “Magnesium Sulfate Attack on Portland Cement Paste – I. Microstructural Analysis”, *Cement and Concrete Research”,* 22 (1992), pp. 169-180.

Bonen. D and Cohen. M.D., “Magnesium Sulfate Attack on Portland Cement Paste – II. Chemical and Mineralogical Analysis”, *Cement and Concrete Research,* 22 (1992), pp. 707-718.

Bukowski J. M. and Berger R. L., "Reactivity and Development of CO_2 Activated Non-Hydraulic Calcium Silicates," *Cement and Concrete Research*, 9 (1979) pp. 57-68.

Duda. A., “Aspects of Sulfate Resistance of Steelwork Slag Cements”, *Cement and Concrete Research*, 17 (1987), pp. 373-384.

Fiori, C., Vandini, M., Prati, S. and Chiavari, G. “Vaterite in the Mortars of a Mosaic in the Saint Peter Basiloca, Vatican (Rome)”, *Journal of Cultural Heritage,* 10 (2009), pp.248-257.

Goto S., Suenaga K., Kado T. and Fukuhara M., “Calcium silicate carbonation products”, J*. Am. Ceram. Soc*. 78 (1995) 2867–2872.

H.F.W. Taylor, Cement Chemistry, 2nd ed., Thomas Telford Publishing, 1997

Huijgen, W. J.J. and Comans, R. N. J. “Carbon Dioxide Sequestration: Literature Review Update 2003 – 2004”. *Report ECN-C-05-022*. Energy Research Center of Netherlands, 2005

Kirboga, S. and Oner, M., “Investigation of Calcium Carbonate Precipitation in the Presence of Carboxymethyl Inulin”, *CrystEngComm,* 15 (2013), pp. 3678-3686.

Lowenstam, H. A. and Abbot, D. P., “Vaterite: A Mineralization Product of the Hard Tissues of a Marine Organism (Ascidiacea)”, *Science,* 188 (1975), pp. 363-365.

Ma, Y. and Feng, Q., “A Crucial Process: Organic Matrix and magnesium Ion Control of Amorphous Calcium Carbonate Crystallization on β-Chitin Film”, *CrystEngComm,* 17 (2015), pp. 32-39.

Popescu, M.-A., Isopescu, R., Matei, C., Fagarasan, G. and Plesu, V., “Thermal Decomposition of Calcium Carbonate Polymorphs Precipitated in the Presence of Ammonia and Alkylamines”, *Advanced Powder Technology,* 25 (2014), pp. 500-507.

Santhanam, M., Cohen, M. D. and Olek, J., “Mechanism of Sulfate Attack: A Fresh Look Part 1: Summary of Experimental Results”, *Cement and Concrete Research,* 32 (2002), pp. 915-921

Słomka-Słupik. B, Podwórny. J and Łukowiec D., “Corrosion of blastfurnace slag paste in aqueous solution of $(NH_4)_2SO_4$”, *Cement Wapno Beton,* 6 (2016), pp. 379-388.

Young J. F., Berger R. L. and Breese J., "Accelerated Curing of Compacted Calcium Silicate Mortars on Exposure to CO_2”, *J. Am. Ceram. Soc*., 57 (1974) pp. 394-397.